ACS OMEGA

http://pubs.acs.org/journal/acsodf

Article

Nonlinear Control of Fouling in Polyethylene Reactors

Fakhrony Sholahudin Rohman, Mohd Roslee Othman, Dinie Muhammad, Ashraf Azmi,* Iylia Idris,* Rushdan Ahmad Ilyas, Samah Elsayed Elkhatif, and Muhammad Nazri Murat*

Cite This: *ACS Omega* 2022, 7, 39648−39661

Read Online

ACCESS | Metrics & More | Article Recommendations

ABSTRACT: Fouling formation in reactor vessels poses a serious threat to the safe operation of the industrial low-density polyethylene (LDPE) polymerization. Fouling also degrades the polymer quality and causes productivity loss to some extent. In this work, neural Wiener model predictive control (NWMPC) is introduced to address the fouling concern. In addition, a soft sensor model is used to activate the fouling−defouling (F−D) mechanism when the fouling surpasses the thickness limit to prevent vessel overheating. NWMPC is proven to be fast, stable, and robust under various control scenarios. The use of a soft sensor model in conjunction with NWMPC enables the online monitoring and controlling of the F−D processes. When comparison is made with a state space (SSMPC) utilizing only the linear block, NWMPC is found to be able to control the LDPE grade with quicker grade transition and lower resource consumption.

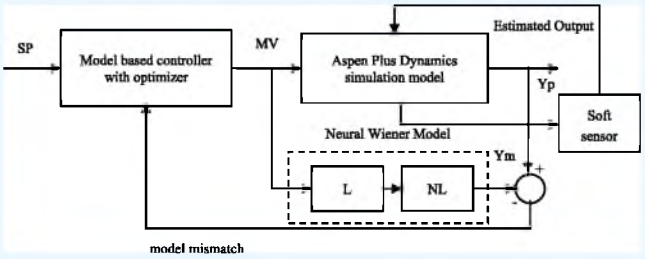

1. INTRODUCTION

Fouling problems arise as a result of the highly exothermic nature of the low-density polyethylene (LDPE) polymerization process and the heating−cooling utilities in tubular reactors (TRs). The polyethylene/ethylene compound shapes two phases inside the reactor, causing fouling in an LDPE-TR.[1] The fouling layer is highly insulating, causing heat transfer restriction to the cooling jacket and thereby reducing the reactor performance. The fouling layer formation can also cause an increase in temperature around the affected location, which can induce the ethylene gas molecule to decompose and liberate a significant amount of heat. The reactor consequently is overheated as the fouling layer thickens over time according to a study by Buchelli et al.[2] This poses a significant threat to the safety in manufacturing facilities.

A high fouling level results in energy losses owing to diminished thermal efficiency and additional capital costs, specifically for the maintenance study, which includes the cleaning of heat transfer (HT) equipment and the use of antifoulants. According to refs 3−6, fouling has various negative consequences, such as abatement in product quality, including the monomer conversion (XM) and melt flow index (MFI). A low manufacturing performance reportedly impacted 0.25 to 30% of the gross domestic product.[7−9] Kiparissides et al.[10] discovered that when fouling builds up, the XM, molecular weight (Mw), long-chain branching (LCB), and density reduce, while the short-chain branching (SCB) and MFI elevate.

Fouling formation on the inner reactor wall is difficult to assess. It has only been described in a few earlier LDPE-related technical papers.[3] Fouling prediction is not systematically formulated in normal practice, and historical data is underutilized for the goal of optimal control.[1] Once the product quality falls outside of the acceptable range, the process parameters are manually adjusted to eliminate fouling and restore the product quality. This manual operation is usually slow and inefficient. The phase equilibria of the polyethylene/ethylene system must be determined to model the fouling mechanism. Fries et al.[11] introduced a fouling model based on the concentration of the foulant in the reactor's local wall cell.

The removal of the fouling layer of polymer adhered to the inside wall of the reactor is referred to as defouling. The defouling method, known as online cleaning, can be used while the plant is still operating. In the functioning of LDPE reactors, a typical fouling−defouling situation occurs. LDPE TRs are subject to periods when the polymer layer is defouled through online pressure cleaning or thermal shock.[2] The reactor fouls in the first period, inducing the values of the fouling thickness layer to rise, while the reactor defouls in the second, leading the fouling thickness layer to fall. Stabilizing the reactor during these disturbance cycles is critical to prevent reactor runaway and maintain the targeted polymer

Received: May 17, 2022
Accepted: September 13, 2022
Published: October 30, 2022

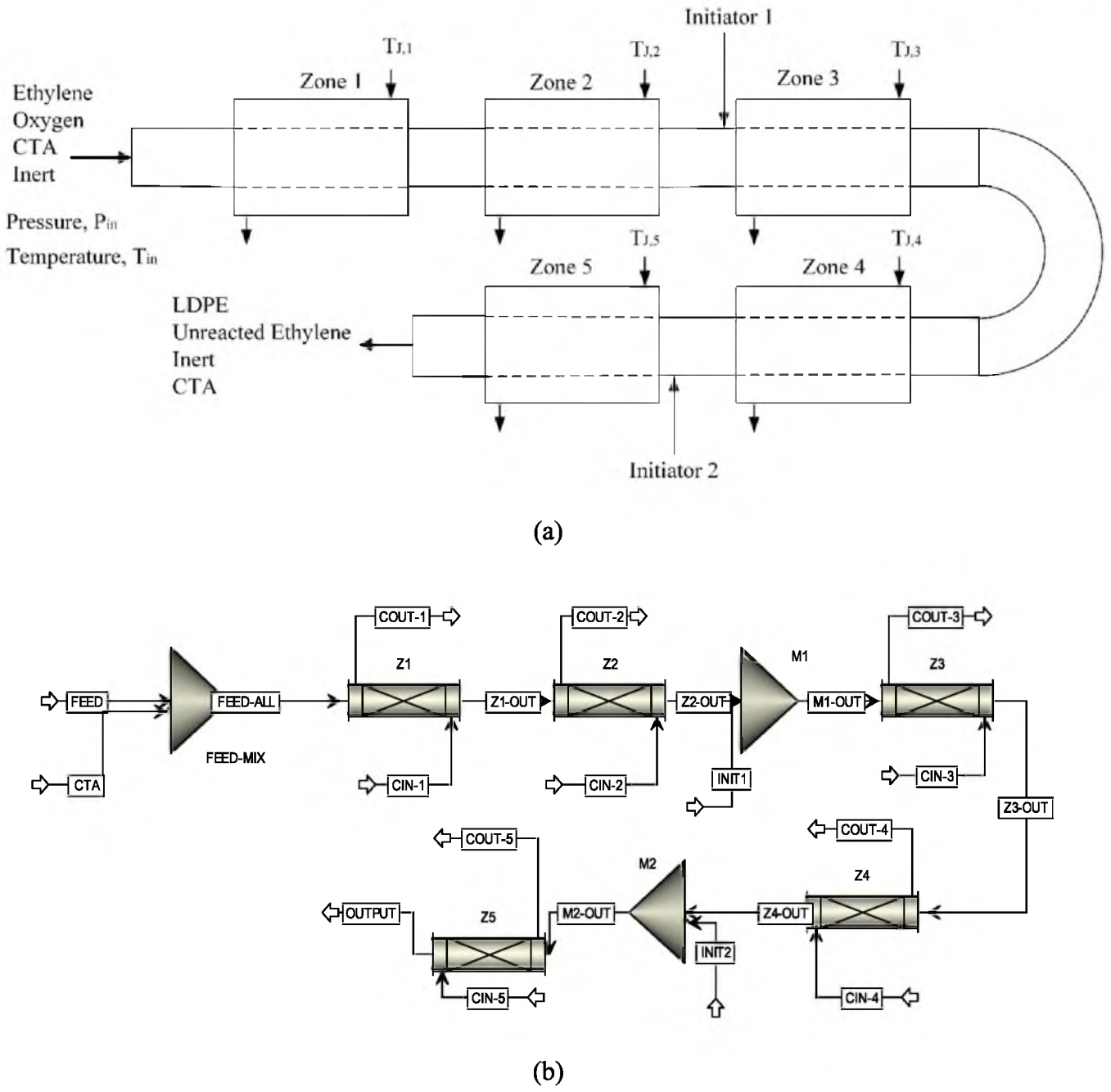

Figure 1. LDPE-TR: (a) schematic diagram of the LDPE TR[32] and (b) Aspen Plus model.

properties. In this scenario, the controller's target is to keep the input profile as close to a specific target profile as possible while the reactor fouls and defouls. Furthermore, the polymer MFI and XM variations should be kept within the acceptable limits.[12]

LDPE reactors are typically made of long pipes (1−3 km) with tiny inner diameters (5−10 cm) and thick reactor walls (2−5 cm) that are separated into several reaction and cooling zones.[13] These multizone arrangements generate strong multivariable interactions along the reactor, resulting in complex operating procedures.[14] One method for regulating the LDPE TR is to use advanced process control (APC), specifically model predictive control (MPC). Due to its intrinsic multivariable control, explicit restriction management, and numerous commercial tools (in modeling and controller implementation), MPC is accepted by in the industry.[15]

The correctness of the process model is critical to the performance of any model-based controller, such as MPC. Since the control of polymer quality in the existence of fouling can be seen as a challenging task in the plant, the LDPE research themes focus primarily on developing a complete polymerization model for predicting polymer quality and fouling[2,16] reactor control,[17] and fouling touchstone monitoring.[2,10]

There are a few studies on LDPE safety control in a fouling−defouling situation. Zavala and Biegler[18] demonstrated that a tracking nonlinear model predictive control (NMPC) can stabilize the reactor in the face of persistent F−D scenarios and that the controller can accomplish strict

https://doi.org/10.1021/acsomega.2c03078
ACS Omega 2022, 7, 39648−39661

control of the MFI. The performance constraints of LDPE reactors in the face of fouling disturbances were evaluated using a first principle model (FPM) of TR. FPM was derived based on the process' mathematical mass, energy, and momentum equations.[19] Nevertheless, its evolution suffers from mathematical complexity as a result of enormous sets of differential and algebraic equations (DAEs). Furthermore, the NMPC cleaning−fouling cycle was simulated using the heuristic mode, in which a single parameter, namely, the heat transfer coefficients (HTCs) for all reactor zones, was scaled from their nominal value. Exogenous disturbances (represented in the model as parameters) are defined when the controller cannot capture the behavior of the HTCs.

It is preferable to set up an efficient strategy for developing online control safety that includes an online fouling−defouling mechanism and an internal model controller development. Although FPM can produce precise prediction, the development of such a model is expensive since it requires maintenance (i.e., dealing with process unknowns), and is only applicable to a particular unique process.[15] The implementation of an empirical model utilizing the nonlinear (NL) model identification technique is an attractive alternative to this challenge.[20] Block-oriented (BO) modeling is one of the existing NL model identification strategies.[21] Furthermore, the identification approach for block-oriented models is convenient as it involves little computational effort, and it allows for the incorporation of existing process knowledge.[22]

The BO (block-oriented) model class includes a variety of configurations, including a linear dynamic system and an NL static element. Wiener's and Hammerstein's models are the most extensively applied block-oriented models. Both models have been used in many case studies and have demonstrated the ability to describe a wide range of NL systems, such as biology and biochemical processes.[23] Because of its transient responsiveness and the dynamic modeling capabilities of its NL portion, the Wiener model is preferable to the Hammerstein model.[24] Several researchers have previously explored the applicability of the Wiener model with NMPC in the literature[25] for online process monitoring.

The development of a soft sensor model can help the online control safety of the LDPE process to activate the defouling action as a certain condition crosses the safety limit by predicting a fouling thickness layer, which can help to capture the fouling−defouling mechanism effectively. The multivariate statistical technique neural network (NN) models such as recurrent network (RN) and multilayer perceptron (MLP) are applicable in soft sensor computational learning.[26,27] Therefore, the application of an NN model for fouling thickness calculation in the LDPE TR is feasible.

The main goal of this work is to develop the neural Wiener-based model predictive control (NWMPC) with an online F−D mechanism as an effective online control safety technique for handling the fouling effect in LDPE TR. In the presence of F−D, the goal of NWMPC is to retain product quality, such as MFI and XM, within strict product specifications. In accordance with the reference value, the MFI variability is fixed at <1%, while the F−D mechanism is activated by controlling fouling thickness. The defouling is activated when the fouling thickness crosses the safety limit (allowable fouling thickness). The novelty of this research is the introduction of NWMPC and fouling thickness estimator combination being applied with the ASPEN simulator as NL controller for handling the fouling of LDPE in TR.

2. MODELING OF THE LDPE TUBULAR REACTOR AND FOULING THICKNESS LAYER

2.1. Process Description. The present LDPE TR model is based on the work of Asteasuain et al.[28] The reactor model is based on an industrial reactor with a huge length/diameter (L/D) ratio of above 20,000 and has been validated using industrial data.[29] The reactor runs at approximately 70 °C at the input to around 325 °C at its peak. The pressure within the reactor is roughly 2200 bar, with a 10% pressure drop throughout the reactor. For the free radical polymerization process to occur in the LDPE-TR, high-temperature and -pressure operations are required. With a mixture velocity of 11 m/s, the reactor residence period is sufficient to ensure that the gel effect phenomenon is negligible inside the wall of the reactor.[30] Figure 1a depicts a schematic diagram of an LDPE TR. According to the figure, the monomer (ethylene) is introduced into the reactor together with oxygen, telogen, and an inert stream. *n*-Butane is used as an inert solvent, whereas oxygen is employed to enhance the polymerization process by producing free radicals,.[31] Propylene is utilized as a telogen or chain transfer agent (CTA) in the mixture to control the production of long polymer chains.[28] Initiators are used to initiate the polymerization process by decomposing into free radicals that bond with ethylene molecules to form active polymer chain molecules. *tert*-Butyl peroxypivalate (TBPPI) is selected as the first initiator, and *tert*-butyl 3,5,5-trimethyl-peroxyhexaonate (TBPIN) is selected as the second initiator.[29,31]

The reactor was composed of five zones for simulation purposes based on the placements of the reactor jacket and initiator. Table 1 describes the reactor's design specifications and nominal operating conditions.

2.2. Reactor Modeling. The model of LDPE TR is developed and validated in this work using the Aspen Plus software. The TR in the Aspen Plus process flowsheet is configured as a collection of RPLUG blocks that indicate the reactor zones (i.e., zone 1, zone 2, zone 3, zone 4, and zone 5).[33] Figure 1b depicts the entire Aspen Plus flowsheet.

Table 1. Tubular Reactor Design Specifications and Nominal Conditions[33]

reactor parameters	values	unit
length/diameter (L/D)	27,800	
internal diameter	0.05	m
number of zones	5	
zone length (L_{zi}, i = 1...5)	60; 100; 180; 510; 540	m
inlet temperature	76	°C
inlet pressure	2250	atm
global heat transfer coefficient (U_i, i = 1...5)	1088.568; 1088.568; 837.36; 628.02; 196.7796	W/m^{2}K
mean jacket temperature (T_{ji}, i = 1...5)	168; 225; 168; 168; 168	°C
density of reacting mixture	530	kg/m^3
monomer flow rate	11	kg/s
oxygen flow rate	6.8×10^{-5}	kg/s
CTA flow rate	7.4×10^{-2}	kg/s
inert flow rate	2.2×10^{-1}	kg/s
initiator 1 flow rate	1.0×10^{-3}	kg/s
initiator 2 flow rate	1.6×10^{-4}	kg/s

https://doi.org/10.1021/acsomega.2c03078
ACS Omega 2022, 7, 39648−39661

Table 2. List of Kinetic Mechanisms and Parameters Used in This Study

kinetic mechanisms	kinetic parameters			efficiency
	k_o (1/s)	E_a (J/kmol)	ΔV (m^3/kmol)	
initiator 1 decomposition (k_i)	1.00×10^{14}	1.3241×10^8	0.0140	0.95
initiator 2 decomposition (k_i)	1.00×10^{12}	1.2393×10^8	0.0116	0.95
oxygen decomposition (k_o)	1.60×10^{11}	1.3361×10^8	−0.0121	0.25
chain initiation (k_{init})	4.00×105	1.7431×10^7	−0.0168	
propagation (k_p)	4.00×10^5	1.7431×10^7	−0.0168	
chain transfer to polymer (k_{tp})	5.20×10^4	3.6844×10^7	−0.0190	
chain transfer to agent (k_{ta})	7.00×10^4	1.8406×10^7	0.0000	
chain transfer to solvent (k_{ts})	7.00×10^4	1.8406×10^7	0.0000	
thermal degradation (k_{thd})	7.70×10^9	8.7430×10^7	−0.0100	
termination by combination (k_{tc})	8.70×10^8	1.5282×10^7	0.0092	
back-biting (k_{bb})	1.20×10^{10}	6.0537×10^7	0.0000	

In the simulation model, initiators 1 and 2 are introduced into the reactor at the start of zones 3 and 5, respectively. The manipulated variable is the CTA flow rate, which is filled independently from the primary feed stream. Perturbed-chain statistical fluid theory (PC-SAFT) equation-of-state (EOS) models specify the thermodynamic characteristics and phase behavior of the LDPE polymerization process.[34] The process heat of polymerization is controlled by regulating the heat of formation (DHFVK) of the polymer segment within Aspen Properties. The DHFVK value specified in this calculation is -2.669×10^7 J/kmol. DHFVK is the heat of formation, which is estimated by using the Van Krevelen Group Contribution Method to estimate the heat capacity and molar volume of the polymer segment (and, thereafter, of polymers and oligomers) inside Aspen Plus. Thus, this work estimates this value using the heat polymerization of ethylene at 21,500 cal/mol[28] via a reverse-calculated method. Thus, the value for DHFVK and heat of polymerization for ethylene is different. The Aspen Plus component database contains all of the components applied in this simulation.

2.3. Kinetic Mechanism. Under high pressure settings, ethylene polymerization proceeded via a free radical mechanism.[35] The LDPE polymerization kinetic mechanism is derived from the mentioned model in Asteasuain et al.,[28] while its characteristics are depicted from the work of Agrawal et al.[31] and Muhammad et al.[33] The LDPE polymerization kinetic process is split into primary reactions: initiator decomposition, chain initiation, chain propagation, chain termination, and chain transfer.[36] The kinetic mechanism used in this work is expressed below:

$$\text{Initiator decomposition} \quad I_{m,i} \xrightarrow{k_i} 2R(0) \tag{1}$$

$$\text{Oxygen decomposition} \quad O_2 + M \xrightarrow{k_o} 2R(0) \tag{2}$$

$$\text{Chain initiation} \quad R(0) + M \xrightarrow{k_{init}} R(m) \tag{3}$$

$$\text{Propagation} \quad R(m) + M \xrightarrow{k_p} R(m+1) \tag{4}$$

Chain transfer to polymer

$$R(n) + P(m) \xrightarrow{k_{tp}} P(n) + R(m) \tag{5}$$

Chain transfer to transfer agent

$$R(m) + S \xrightarrow{k_{ts}} P(m) + R(0) \tag{6}$$

$$\text{Chain transfer to solvent} \quad R(m) + S \xrightarrow{k_{ts}} P(m) + R(0) \tag{7}$$

Termination by combination

$$R(n) + R(m) \xrightarrow{k_{ts}} P(n+m) \tag{8}$$

$$\text{Thermal degradation} \quad R(m+1) \xrightarrow{k_{thd}} P(m) + R(0) \tag{9}$$

$$\text{Back} - \text{biting} \quad R(m) \xrightarrow{k_{bb}} R(m) \tag{10}$$

The modified Arrhenius equations are used in Aspen Plus to compute the kinetic rate constants for the free radical reaction, as seen in eq 11:

$$k = k_o \exp\left[-\left(\frac{E_a}{R} + \frac{\Delta V \times P}{R}\right)\left(\frac{1}{T} - \frac{1}{T_{ref}}\right)\right] \tag{11}$$

Table 2 shows the LDPE kinetic mechanisms and properties considered in this study. Because the referred work uses different modeling techniques than Aspen modeling, the kinetic rate constants must be tuned specifically.[34] To supply the reactor temperature profile, the efficiency of the initiators and oxygen has been retuned using the Aspen Data Fitting technique. Furthermore, Aspen Design Spec was utilized to compute the activation energy of the beta scission reaction to achieve the average LDPE's Mw.

2.4. Melt Flow Index Model. The MFI values in this study are calculated using Rokudai and Okada's[37] empirical formulation, as shown in eq 12:

$$\text{MFI} = 1.06 \times 10^{28} (\tilde{g} \times \text{MWW})^{-6.06} \tag{12}$$

Based on many studies in estimating MFI for LDPE,[12,37] the main prerequisite for estimating it is the weight average molecular weight and branching index information. The branching index determined from Dietrich et al.,[38] a comprehensive study of the similarly referred LDPE model, is denoted by the value of $\tilde{g}$. Because the LDPE polymer comprises complex branches, the branching index information is indispensable; otherwise, no prevalent relationship can be determined until the polymer's rheology is characterized.[39] The weighted average molecular weight (MWW, kg/kmol) is derived in the Aspen simulation model utilizing the method of moments. The Aspen Plus Dynamics model is attached with the MATLAB Simulink environment to execute the equation. The Aspen Plus Dynamics model is processed as a simulation block on the MATLAB Simulink environment, and its output

https://doi.org/10.1021/acsomega.2c03078
ACS Omega 2022, 7, 39648−39661

(MWW) is computed using an approximation branching index to determine the MFI values.

2.5. Reactor Model Validation. The validation results of the reactor temperature profile according to zones are shown in Figure 2. From the figure, the Aspen Plus model effectively

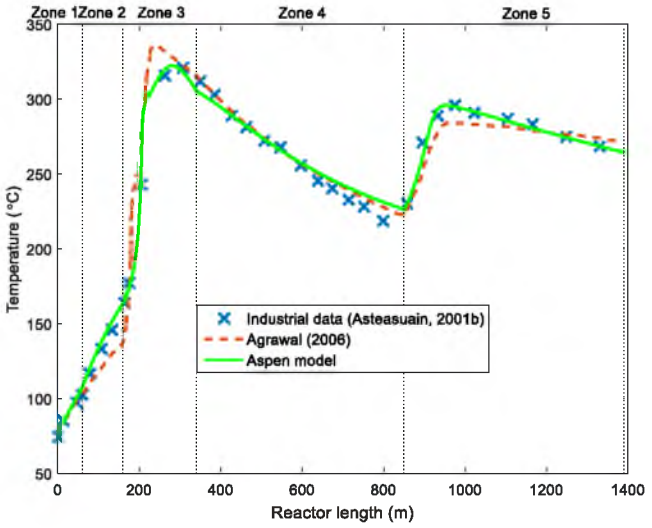

Figure 2. LDPE reactor temperature validation profile.

generates the reactor temperature profile with an R^2 value of 0.981, which compares well with the industrial data provided by Asteasuain et al.[28] Furthermore, the simulated temperature profiles resemble the temperature profiles of industrial reactors, which have a rounded peak and a gradual decline.[34] It is noteworthy that the Aspen Plus model outperforms the mechanistic model from Agrawal et al.,[31] which also used a similar case study, in predicting the reactor temperature profile. This is because the Aspen model used a fine-tuning procedure for the kinetic parameters.

Table 3 summarizes the results of the LDPE final XM and property validation. The table compares industry data with the

Table 3. LDPE XM and Property Validation

properties	industrial data Asteasuain et al. (2001)[28]	Agrawal et al. (2006)[31]	error (%)	Aspen Model	error (%)
XM (%)	30.0	29.7	1	29.5	1.7
number average Mw (g/mol)	21,900	21,901	0<	22,070	0.8
mixture density (g/mL)	0.530	n/a		0.565	6.6

Aspen Plus model and the Agrawal model[31] in terms of LDPE XM, average Mw, and mixture density. According to the table, the developed model correlates favorably to the industrial data.[28] The accuracy of the developed model to describe the LDPE-TR is high as a result of the temperature and property validation results.

2.6. Formation of the Fouling Thickness Layer. The fouling resistance (t_f) is calculated using the condition of overall heat transfer coefficients (U, W/m^{2}K). There are two primary ways for determining U: first, U_{clean} using correlations[2] and second, using heat transfer system data from a plant. The first technique relies on correlations of dimensionless numbers derived from the component's physical characteristics and operating conditions. The second method calculates U_{plant} using the heat transferred and the log mean temperature discrepancy. Because plant data obviously demonstrates a fouling behavior in the reactor, the fouling thickness in the LDPE-TR can be examined using U_{plant} and a heat-transfer model.[2]

As shown in the equation below, the equation for U takes four resistances into account in series: those of the film on the reaction mixture side, the reactor wall, the film on the cooling/heating jacket side, and the fouling buildup, R_f (fouling resistance, m^2 K/W). In this study, the effects of film and thermal resistance are considered to be constant throughout the study. Thus, these assumptions (and limitations) were applied in this study. It is worth noting that the U coefficient is affected by variables that are computed as functions of the time:

$$\frac{1}{U(t)} = \frac{1}{h_i(t)} + \frac{2.3D}{2k_w}\log_{10}\left(\frac{D_0}{D}\right) + \frac{1}{h_j(t)\left(D_0/D\right)} + R_f(t) \tag{13}$$

where D_0 and D are the internal diameters of the jacket and reactor, respectively, and k_w is the thermal conductivity of the wall. Lacunza et al.[40] provide a review of HTC used in ethylene polymerization. Calculating U under clean conditions is possible with R_f = 0. Using eq 14, the HTC can be calculated directly using the temperature differences and heat transferred in the reactor.

$$U_t = \left(\frac{Q}{A\Delta T_{lm}}\right)_t \tag{14}$$

According to Buchelli et al.,[2] the evaluation of the fouling mechanism can be attained at a maximum in the cooling zone's terminal point. The U value is lower when the surface is fouled. Equation 15 is used to calculate the fouling resistance (R_f) value.

$$R_f = \left(\frac{1}{U}\right)_{fouled} - \left(\frac{1}{U}\right)_{clean} \tag{15}$$

where U_{fouled} refers to U_{plant} in Equation, whereas U_{clean} refers to U in the equation with R_f = 0. The foulant resistance is related to a foulant thickness (mm), t_f given in eq 16, assuming that the foulant is the polymer attached to the wall.

$$R_f = \left(\frac{1}{k_{polymer}}\right)(r_i - t_f)\ln\left(\frac{r_i}{r_i - t_f}\right) \tag{16}$$

$$k_{polymer} = 0.274 + 2.91 \times 10^{-5} \times P + \frac{10.47}{T} \tag{17}$$

where $k_{polymer}$ (W/m·K) is the polymer thermal conductivity and r_i (m) is the inside reactor radius. The heat transfer coefficients U (W/m^{2}K) and temperature T (K) inputs of the equation have a significant effect on t_f, such as shown in Figure 3. In the meantime, the pressure P (N/m^2) remained almost constant throughout the course. Based on the study of Buchelli et al.,[2] the fouling layer's rise appears to be linear over time with 0.00004 kg/s of calculated deposition rate followed by a decrease of 2.083 × 10^{-5} mm/s fouling thickness after defouling. To determine t_f in eq 16, a direct analytical approach is infeasible. It can be solved numerically to develop an approximation model. As a consequence, the

https://doi.org/10.1021/acsomega.2c03078
ACS Omega 2022, 7, 39648−39661

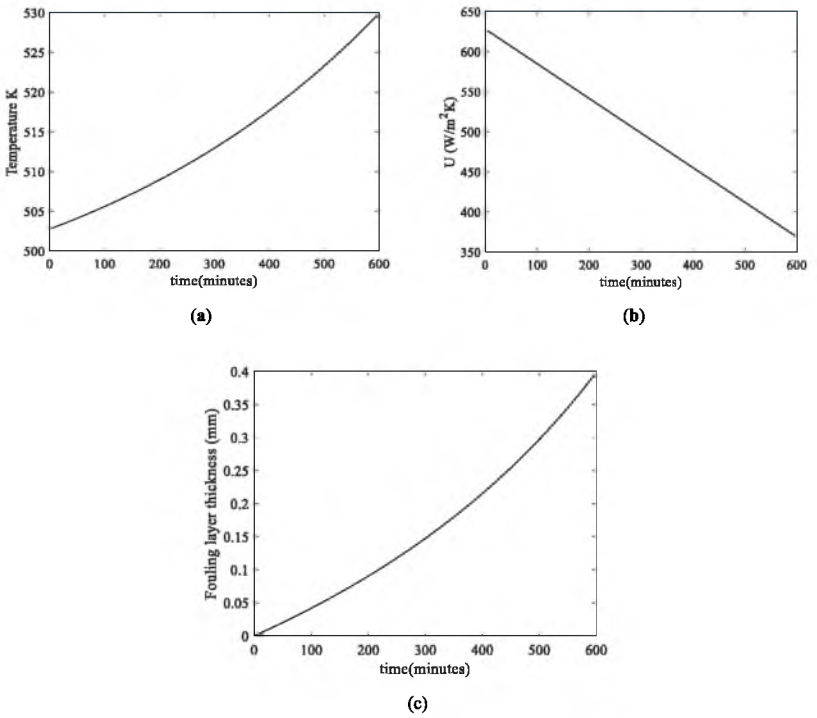

Figure 3. The validated data (a) U and (b) T depicted from Aspen Plus with the (c) calculated t_f.

empirical model of t_f with the input functions of U and T is formulated as

$$t_f = 0.0006273\frac{T}{U} - 0.0004996 \tag{18}$$

The validated data (U and T) from Aspen plus and the t_f from the empirical model are considered actual data, which are then used to develop the soft sensor model.

3. SOFTWARE SENSOR FOR ESTIMATING FOULING THICKNESS

The soft sensor model is built using the MATLAB neural network (NN) identification technique. The FFNN (feed forward neural network) model is extensively implemented in chemical processes and engineering applications, attesting to its ability to model NL systems.[41,42] The NN model is trained using the *trainlm* function in MATLAB, which is known as Levenberg–Marquardt (LM) backpropagation. LM training is the fastest available backpropagation technique available in MATLAB. The MISO model is used in the development of soft sensors. In this case, the holdout method is used for the model cross-validation. First, 70% of the data is used during the training process. Then, 15% of the data is employed for validation during the training process (to prevent overfitting). Finally, the rest of the data (15%) is used for the second validation after the training is completed. To evade ill-conditioned system modeling, all parameters are reformed by data scaling using eq 19 below:[43]

$$x_{scaled} = \frac{x - x_{ss}}{x_{max} - x_{min}} \tag{19}$$

where x is the original value, x_{ss} is the steady-state value of the parameter, x_{max} is the maximum value of the parameter, and x_{min} is the minimum value of the parameter. The maximum and minimum values are determined from this work parametric analysis.

Table 4 lists the parameters for the soft sensor model. The input parameters are listed in the order in which data measurements from the Aspen Plus Dynamics model are available. An input selection methodology is devised to select the appropriate inputs for the soft sensor model.

Table 4. Parameters for Soft Sensor Model Input–Output Selection

input parameters	output parameter
initiator 1 flow rate	fouling thickness
initiator 2 flow rate	
CTA flow rate	
heat transfer coefficient in zone 3	
heat transfer coefficient in zone 4 (cooling)	
heat transfer coefficient in zone 5	
temperature of terminal point zone 3	
temperature of terminal point zone 4 (cooling)	
temperature of terminal point zone 5	
polymer exit density	

The software sensor inputs (ANN model) are chosen using the Pearson correlation coefficient (PCC) analysis. PCC is a technique for selecting variables based on linear correlation of the respective variables.[44] The PCC results are listed in Table 5. The higher PCC value shows the higher correlation or relationship of the input parameter with the output parameter.

Here, U, T, and polymer density are excited with minimum and maximum changes from their steady-state value using a uniform random number generator. For each model training and validation purpose, 800 min of simulation time with a sampling time of 0.1 min and a total of 8000 data points was applied for building the NN model. Figure 4a–c depicts the outcomes of input excitation from U, T in the cooling zone, and polymer density under the specified range operating condition. The regression plot for the NN model with the

https://doi.org/10.1021/acsomega.2c03078
ACS Omega 2022, 7, 39648–39661

Table 5. PCC Results for Parameter Outputs

input parameters	PCC fouling thickness
initiator 1 flow rate	0.278
initiator 2 flow rate	0.127
CTA flow rate	0.277
heat transfer coefficient in zone 3	0.188
heat transfer coefficient in zone 4 (cooling)	**0.993**
heat transfer coefficient in zone 5	0.012
temperature of terminal point zone 3	0.231
temperature of terminal point zone 4 (cooling)	**0.970**
temperature of terminal point zone 5	0.302
polymer exit density	**0.721**

best hidden neurons is shown in Figure 5. According to the figure, the model has a high correlation with the target data and a low disparity. The model fouling thickness has an R^2 value of 0.999. Thus, with these validation results, the model is found to be suitable for use in a soft sensor model study.

4. DEVELOPMENT OF ONLINE SAFETY CONTROL USING MPC

To connect the MATLAB Simulink environment with Aspen Plus Dynamics, the online safety control system is linked using (Aspen Modeler) AMSimulation. Figure 6a shows the implementation of the NW model in the MPC control scheme. Figure 6b depicts a generic block diagram of the model predictive control (MPC) workflow for online safety control.

When contrasted to the actual process by the Aspen Plus Dynamics model, the internal model works as the ideal process condition. Neural Wiener (NW) and state space (SS) are the internal models investigated in this study. A model mismatch is the difference between the two outputs, which is produced by process disturbance or uncertainty. A set point (or reference) signal is delivered to the controller to indicate the model mismatch. The model mismatch signal indicates the current state of the process, while the set point signal represents the desired state of the process. Both signals are generated using an optimization strategy within the MPC algorithm to create the optimal process input that can lead the process to the target condition. The soft sensor monitors the fouling thickness dynamic, which triggers the defouling scenario when the fouling thickness exceeds the permissible maximum value, $t_f > 3.5$ mm. The defouling scenario is carried out by online cleaning for approximately 4 h, as noted by an increase in U value and a decrease in t_f.

The development of the neural Wiener MPC (NWMPC) in this work follows a structure that is similar to that of the given MPC scheme but with a few transformations. To begin, the output measurement is utilized to immediately update the process model without the requirement of an observer because the Aspen model can give process state measurements. Second, in the optimizer's cost functional algorithm, the current controller utilizes just output reference tracking and modifications in manipulated variables. Generally, MPC can control the process with these two cost functions satisfactorily.[45] These cost functions are resolved via an online optimization approach to deliver the trajectory of the controller output. The selection of the process model type is the primary factor that distinguishes nonlinear MPC (NMPC) from linear MPC (LMPC). The NMPC uses the neural Wiener (NW) model as its process model in this study, which is referred as neural Wiener MPC (NWMPC).

In this scheme, three MVs (initiator 1, initiator 2, and CTA flow rate) are utilized to control two CVs (LDPE XM and MFI), resulting in a multi-input multi-output (MIMO) system. In addition, the NW model block serves as the

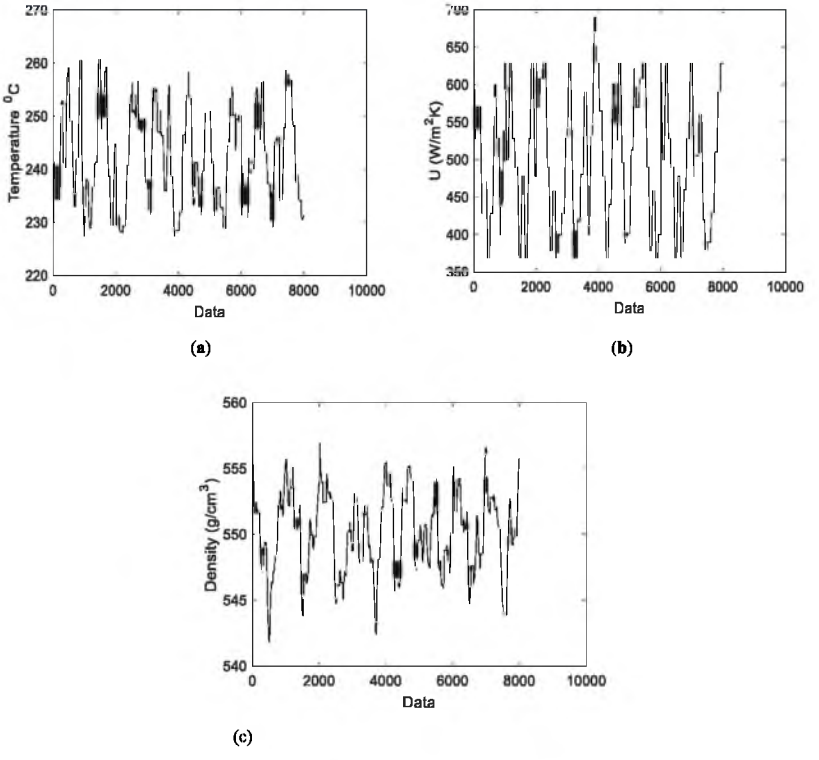

Figure 4. Process input excitation data: (a) U, (b) T in the cooling zone, and (c) polymer density.

https://doi.org/10.1021/acsomega.2c03078
ACS Omega 2022, 7, 39648−39661

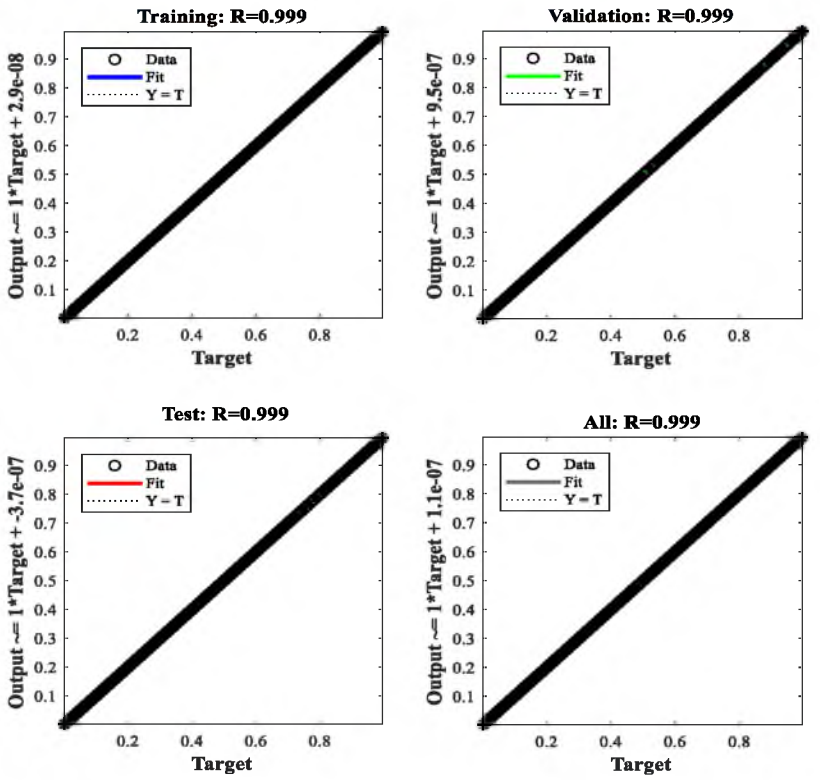

Figure 5. Regression plot for fouling thickness.

MPC process model, inducing model mismatch that updates the MPC controller at each sampling period. SSMPC is also designed to compare the performance using a similar control scheme. By switching the NW model for the SS model, the SSMPC control scheme can be acquired.

4.1. Identification Technique. The Weiner model identification using the linear−nonlinear (L−NL) technique is used in this research.[46] In accordance with the method, the first step is to collect a set of dynamic data. To obtain this data, perturbations of the Aspen Plus Dynamics model are carried out. The intermediate signal is then specified as the data set's output. A Wiener model linear block can be represented by the state space model as follows:

$$x(k+1) = \boldsymbol{A}x(k) + \boldsymbol{B}u(k)$$
$$v(k) = \boldsymbol{C}x(k) \tag{20}$$

Once the linear block has been identified, the model output signal is used as the input signal for the NW static NL block identification. In this scenario, the identification of NL processes is performed using the MATLAB NN toolbox and a single layer feed forward fitting NN (*fitnet*) model. The output of the NN model, $y(k)$, is written as follows:

$$y(k) = w_0 + \sum_{i=1}^{K} w_i^2 \boldsymbol{\varphi}(z_i(k)) \tag{21}$$

where

$$z_i(k) = w_{i,0}^1 + w_{i,1}^1 v(k) \tag{22}$$

In the equation, the network bias is represented by w_0, and the network weight is specified by $w_{i,j}^1$ and $w_{i,j}^2$ for the first and second layers, respectively. In addition, $v(k)$ represents the state space model output signal, φ denotes the network NL transfer function (i.e., hyperbolic tangent sigmoid), and K signifies the number of hidden nodes.

To determine the number of hidden nodes, the iterative validation approach is used. The NN model is trained using Levenberg−Marquardt (LM) backpropagation, and an early stopping mechanism is utilized to avoid the network from overfitting during the training process. The ultimate result of the NW model is exhibited as follows:

$$y(k) = w_0 + \sum_{i=1}^{K} w_i^2 \boldsymbol{\varphi}(w_{i,0}^1 + w_{i,1}^1 [Cx(k)]) \tag{23}$$

4.2. Controller Development. In this paper, the optimizer of the NWMPC controller employs sequential quadratic programming (SQP). The MATLAB optimization tool *fmincon* function is used to run the SQP optimization program. The quadratic objective function used in the MPC control scheme is presented in eq 24.

$$\min_{\Delta u(k)} J = \sum_{i=1}^{p} \{W_y[\hat{E}(k+i)]\}^2 + \sum_{i=0}^{P-1} \{W_u[u(k+i) - u(k+i-1)]\}^2 \tag{24}$$

The predicted error term, $\hat{E}$, can be defined (for next prediction horizon step) as follows:

$$\hat{E}(k+1) \triangleq Y_r(k+1) - \tilde{Y}(k+1) \tag{25}$$

where Y_r is the desired set point and $\tilde{Y}$ is the corrected prediction over the prediction horizon, P. $\tilde{Y}$ can be acquired by:

$$\tilde{Y}(k+1) \triangleq \hat{y}(k+1) + \boldsymbol{\varepsilon}(k+1) \tag{26}$$

https://doi.org/10.1021/acsomega.2c03078
ACS Omega 2022, 7, 39648−39661

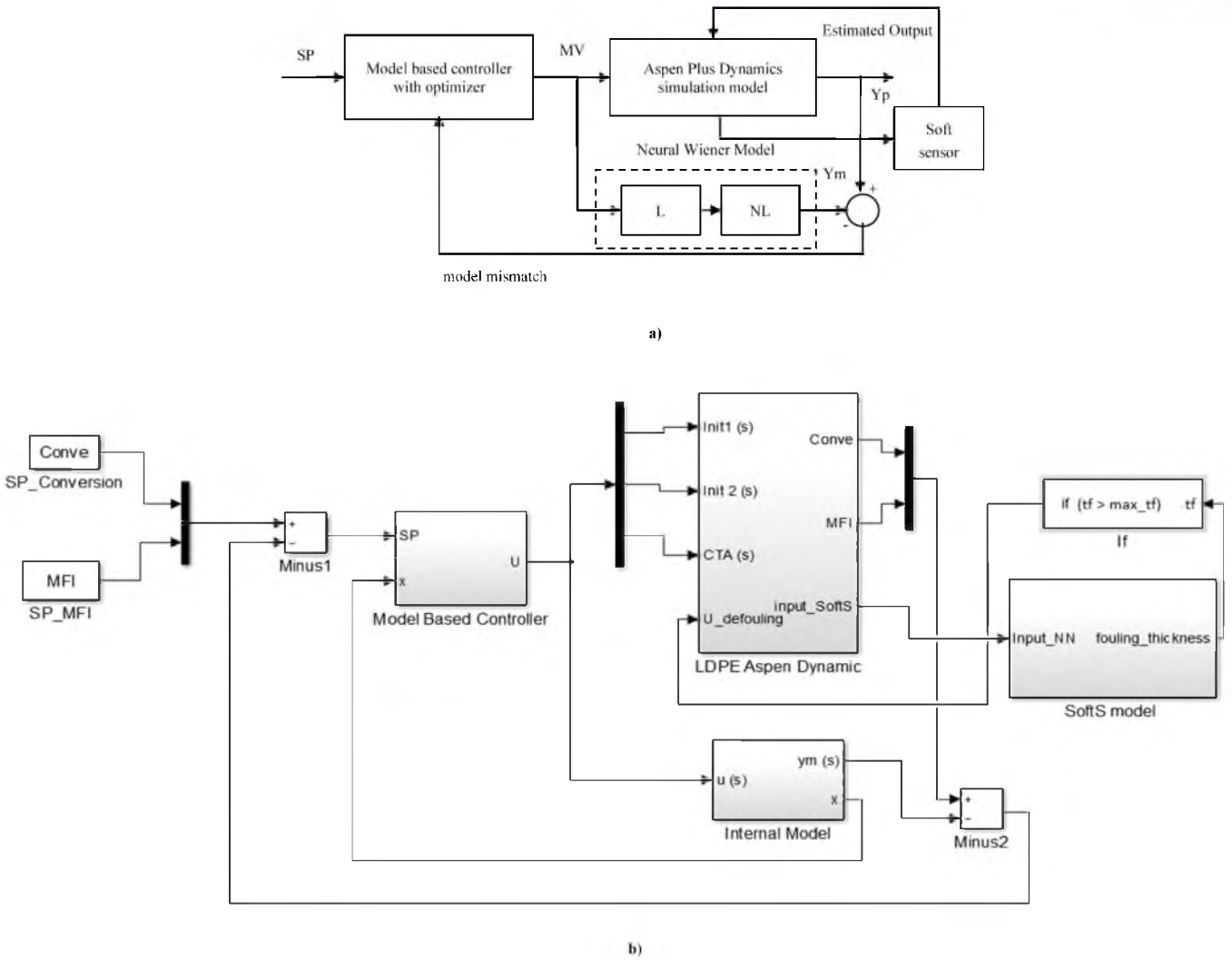

Figure 6. Scheme diagram of MPC: (a) neural Wiener model in NMPC control scheme and (b) online control safety scheme with Aspen Plus Dynamics inside MATLAB Simulink.

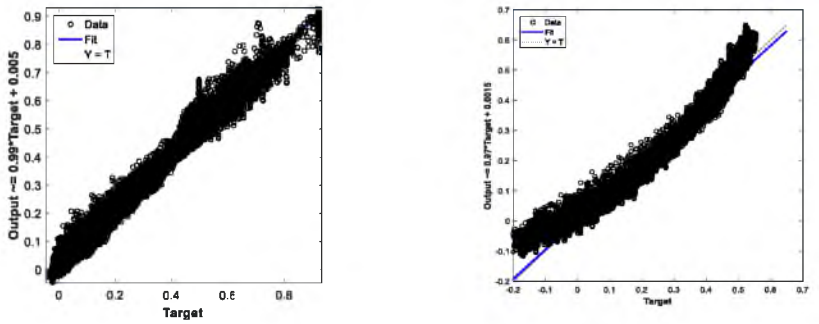

Figure 7. Regression plot for LDPE XM (Y1) for the (a) neural Wiener model (b) state space model.

where $\hat{y}(k+1)$ is referred to as uncorrected prediction and $\epsilon(k+1) = y(k) - y_m(k)$ is the model mismatch term.

4.3. Tuning Method. The prediction horizon (P), control horizon (M), output weighting (or error penalty) matrix, and input rate weighting (or move suppression) matrix are the four tuning parameters for a specific MPC. The guidelines of Seborg et al.[47] are used to select the prediction and control horizon settings. The rules are $5 \leq M \leq 20$ and $N/3 < M < N$, where N represents the model horizon. The model horizon can be determined using $N\Delta t = t_s$, where Δt is the sampling time and t_s is the settling time of the open-loop response. When the control horizon M is expanded, the MPC gets more rigorous, which necessitates greater computational work. To account for the complete influence of the most recent input motion, the prediction horizon is usually set to $P = N + M$. As the control horizon decreases, the controller becomes more rigorous.

https://doi.org/10.1021/acsomega.2c03078
ACS Omega 2022, 7, 39648−39661

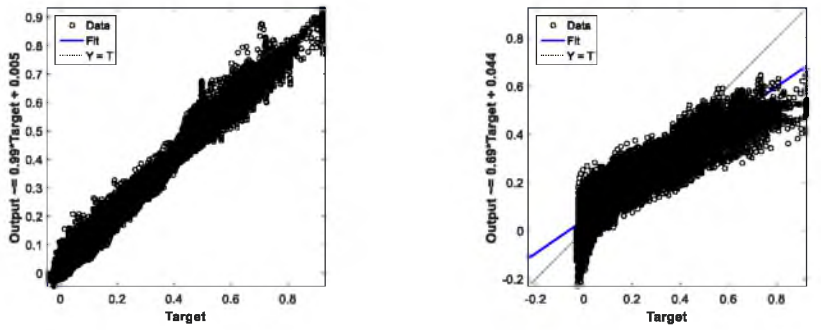

Figure 8. Regression plot for MFI (Y2) for the (a) neural Wiener model (b) state space model.

After the P and M parameters have been finalized, the MPC controller is tuned using the MATLAB MPC Tuning Advisor based on a linear version of the process. The output weighting and input-rate weighting matrix in the software are modified to yield the best performance using the Integral Absolute Error (IAE) performance indicator. After obtaining an acceptable performance with the tuning software, the initiatory tuning settings are re-evaluated during the online closed-loop simulation. At this phase, the controller is improved using a heuristic technique, with only the output tuning weight that is changing.[48]

5. RESULTS

5.1. Model Identification Results. Each training and validation data set has yielded a total of 4080 min of LDPE TR simulation results. Excitation inputs include the initiator 1 flow rate, initiator 2 flow rate, and CTA flow rate, as well as response, LDPE XM, and MFI outputs in each data set. The identification of the neural Wiener model involves two different model identification processes: state space and NN identification. The model order is determined using Hankel singular values during state space model identification. The state space model of the sixth order is determined based on the Hankel singular value test. The number of hidden neurons chosen for the NN model is nine, which has the lowest mean square error (MSE) from the validation data test. Figure 7 depicts the NW model identification results as a regression plot. According to the figure, the majority of the output data agrees with the target (validation) data based on the low disparity distribution of the data points along the fit line. The coefficient of determination (R^2) analysis is used to evaluate the model's performance. According to the figure, both parameters fit the validation data well, with an R^2 value of 0.989 for LDPE XM and R^2 value of 0.986 for MFI output. In the NWMPC control scheme, the validated NW model can be implemented as the process model.

The results for SS and neural Wiener (NW) model identification display the LDPE XM and MFI in a scaled form, respectively. The steady-state condition is represented by the value "0". MATLAB calculates the fit line, which represents the linear correlation of both data. According to Figure 7a, the NW model's output data is spread more imminently throughout the diagonal line ($Y = T$) than the SS model. This indicates that the estimation from the NW model fits the original data better than the SS model. The SS model has drawbacks in capturing the maximum and minimum region of the data, as evidenced by its imprecise data distribution at both extremities in Figure 7b. Based on R^2 calculations, the NW model has $R^2 = 0.9889$, which is higher than the SS model, which has $R^2 = 0.9509$.

Figure 8 depicts the regression plots of the NW and SS models for predicting MFI values. In comparison to the SS model, the NW model output data distribution is denser along the fit line, as shown in the figure. The residuals in the SS model output data are higher, spreading widely from the fit line and being congested at the minimum values. Thus, the NW model outperforms the SS model in predicting MFI values, with $R^2 = 0.9860$ versus $R^2 = 0.6693$ for the linear model.

5.2. Online Safety Control Results. In this case, the NWMPC controller is tested in a grade transition under fouling and F−D conditions. These tests are carried out to evaluate the controller in terms of tracking set points and handling process uncertainties in the presence of a fouling effect. A state space MPC (SSMPC) is used as a comparison to assess the performance of the NWMPC controller. The SSMPC is created by utilizing only the linear block (i.e., state space) of the NW model.

Aspen Plus Dynamics is used to simulate the LDPE TR model, which runs concurrently with MATLAB Simulink during the simulation. Table 6 displays the tuning outcomes for SSMPC and NWMPC. The initial tuning parameters of the MPC controllers are derived via calculation[47] and offline simulation with the MATLAB MPC Tool.

Table 6. MPC Tuning Parameters

parameters	SSMPC	NWMPC
prediction horizon (P)	45	45
control horizon (M)	5	5
output weighting	0.11, 0.09	1.1, 2.0
input rate weighting	1.5, 1.2, 1.2	1.5, 1.2, 1.2

5.2.1. Grade Transition under a Fouling Effect. The process of changing the operating parameters of a reactor to a specific polymer grade based on a predetermined product recipe is known as grade transition. Figure 9 depicts the performance of the SSMPC and NWMPC in handling the step change grade transition operation in the presence of a fouling effect. According to Figure 9a, NWMPC reaches new grade MFI faster and with a quicker rise time than SSMPC. The fast CTA controller is set in the first 20 min (refer to Figure 9b for the MV profile). Because there is a rate limitation on the CTA flow rate, NWMPC decreases the flow rate of its initiators, as shown in Figure 9d,e.[49] Polymer MFI can be enhanced by lowering initiator flow rates. Furthermore,

https://doi.org/10.1021/acsomega.2c03078
ACS Omega 2022, 7, 39648−39661

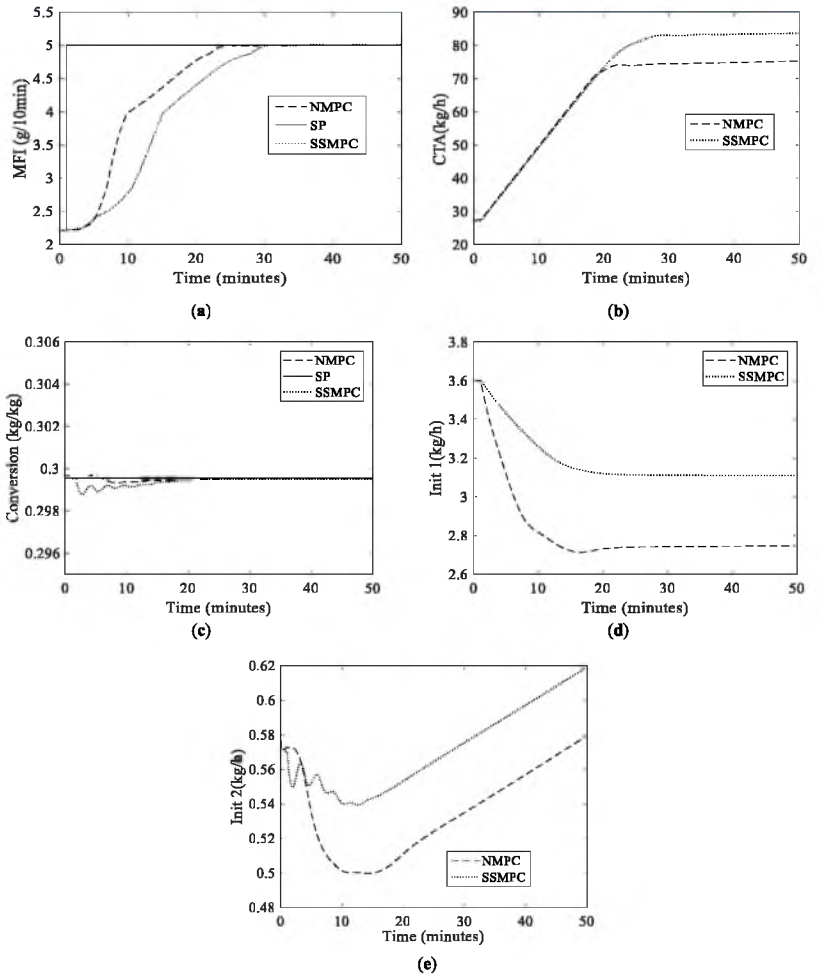

Figure 9. Comparison of grade transition control for NWMPC and SSMPC: (a) MFI profile, (b) CTA flow rate profile, (c) conversion profile, (d) initiator 1 flow rate profile, and (e) initiator 2 flow rate profile.

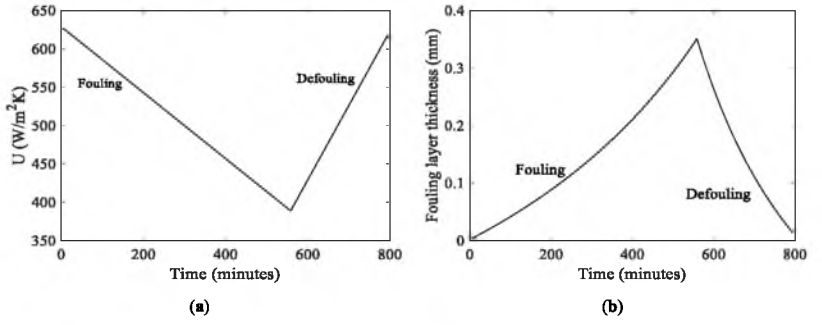

Figure 10. Heat transfer coefficient (a) and estimated fouling thickness (b) under the fouling−defouling scenario.

as shown in Figure 9b, the decrement in initiator flow rates has a little effect on LDPE conversion. Based on the error analysis, NWMPC produces IAE values of 4.937 and 0.0683, respectively, for the MFI and LDPE conversion profiles, while SSMPC produces IAE values of 7.609 and 0.013. As a result, NWMPC is able to control the LDPE grade transition using optimized controller outputs, allowing for quicker grade transition and lower resource consumption (CTA and initiators).

In terms of control stability and feasibility of the NWMPC, the Karush−Kuhn−Tucker (KKT) conditions are evaluated. Since the optimization process (in the controller) is performed successfully in the MATLAB Simulink environment, the KKT conditions have been met. Thus, it is safe to say that the control scheme is also stable and feasible.

5.2.2. Fouling−Defouling Mechanism. Figure 10 depicts the estimated heat transfer coefficient (HTC) and fouling thickness of a fouled TR under an F−D scenario. The HTC decreases on a regular basis as fouling accumulates with increasing fouling thickness. When the fouling thickness, t_{fj} reaches the maximum limit of 0.35 mm at 497 min, the defouling mechanism activates the online cleaning to reduce fouling t_{fj}, thereby improving heat transfer.

The effect of F−D on the reactor outputs and MV profile is shown in Figure 11. Both controllers are able to tackle the F−D condition, as shown in Figure 11a, with SSMPC displaying

https://doi.org/10.1021/acsomega.2c03078
ACS Omega 2022, 7, 39648−39661

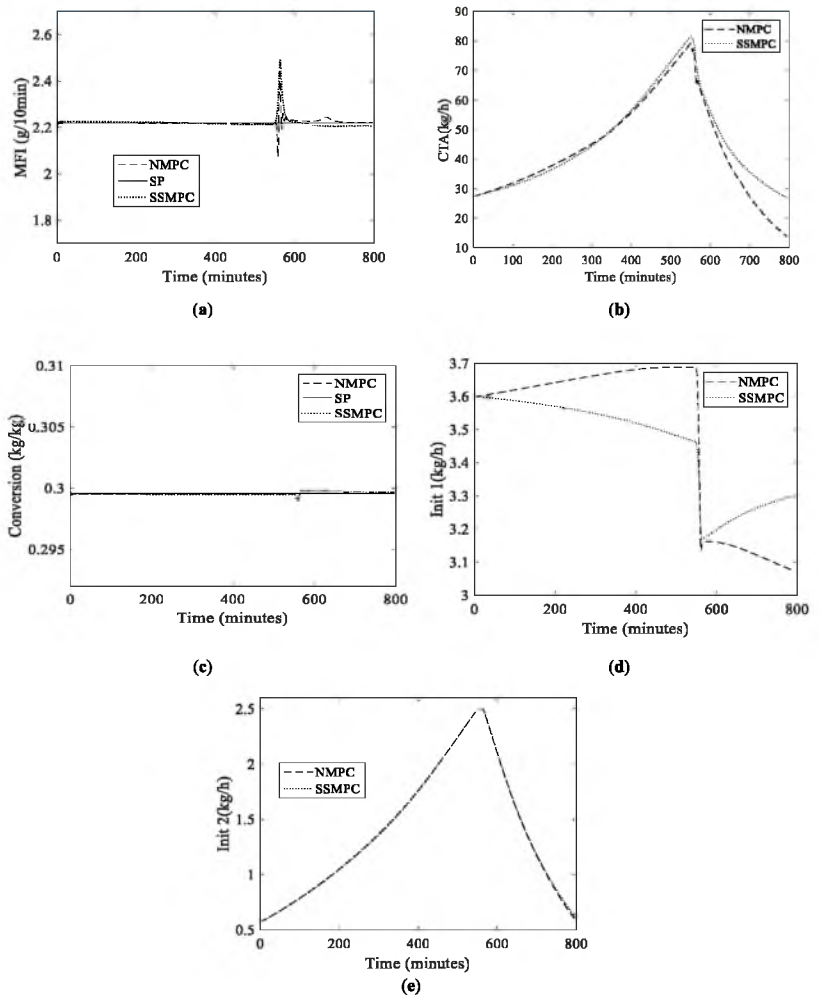

Figure 11. Comparison of fouling−defouling control for NWMPC and SSMPC: (a) MFI profile, (b) CTA flow rate profile, (c) conversion profile, (d) initiator 1 flow rate profile, and (e) initiator 2 flow rate profile.

a minor divergence in the MFI profile. In the MFI profile, NWMPC generated an IAE value of 4.937 compared to SSMPC's ISE value of 7.609. In Figure 11c, both controllers perform similarly in terms of polymer XM maintenance despite the fact that NWMPC uses more initiator than SSMPC (see Figure 11d). Based on the error analysis in the XM profile, both controllers produce comparable IAE, with NWMPC 0.0683 and SSMPC 0.0919. Similar findings can be found in the study of Zavala and Biegler[18] of NMPC performance in the presence of F−D inside an LDPE TR. As a result, the controllers demonstrate a successful activation of the F−D mechanism within the reactor.

6. CONCLUSIONS

The development and performance evaluation of the neural Wiener MPC (NWMPC) in regulating a high-pressure LDPE TR are presented. A soft sensor model is developed with the NWMPC control scheme (NWMPC-SS) to address the fouling and defouling operation in the plant. This control system is crucial because it offers the required stability and security for safe plant operation. In the LDPE TR, the NWMPC is proven to be fast, stable, and robust under various control scenarios. The use of a soft sensor model in conjunction with NWMPC enables the online monitoring and controlling of the F−D processes. The soft sensor model is added to the NWMPC control scheme separately and can be operated independently if necessary. The NWMPC-SS demonstrates its control solution for NL processes in the polymer industry with safety concerns.

AUTHOR INFORMATION

Corresponding Authors

Ashraf Azmi − *School of Chemical Engineering, College of Engineering, Universiti Teknologi MARA, Shah Alam 40450 Selangor, Malaysia*; orcid.org/0000-0003-1030-4350; Email: ashraf.azmi@uitm.edu.my

Iylia Idris − *School of Chemical Engineering, College of Engineering, Universiti Teknologi MARA, Shah Alam 40450 Selangor, Malaysia*; Email: iyliaidris@uitm.edu.my

Muhammad Nazri Murat − *School of Chemical Engineering, Engineering Campus, Universiti Sains Malaysia, Nibong Tebal 14700 Penang, Malaysia*; Email: chnazri@usm.my

Authors

Fakhrony Sholahudin Rohman − *School of Chemical Engineering, Engineering Campus, Universiti Sains Malaysia, Nibong Tebal 14700 Penang, Malaysia*

Mohd Roslee Othman − *School of Chemical Engineering, Engineering Campus, Universiti Sains Malaysia, Nibong Tebal 14700 Penang, Malaysia*; orcid.org/0000-0002-3191-2358

https://doi.org/10.1021/acsomega.2c03078
ACS Omega 2022, 7, 39648−39661

Dinie Muhammad − *School of Chemical Engineering, Engineering Campus, Universiti Sains Malaysia, Nibong Tebal 14700 Penang, Malaysia*
Rushdan Ahmad Ilyas − *School of Chemical and Energy Engineering, Faculty of Engineering and Centre for Advanced Composite Materials (CACM), Universiti Teknologi Malaysia (UTM), Johor Bahru 81310 Johor, Malaysia; Institute of Tropical Forestry and Forest Products, Universiti Putra Malaysia (UPM), Serdang 43400 Selangor, Malaysia*
Samah Elsayed Elkhatif − *Mechanical Engineering, Faculty of Engineering and Technology, Future University in Egypt, New Cairo 11845, Egypt*

Complete contact information is available at: https://pubs.acs.org/10.1021/acsomega.2c03078

Notes

The authors declare no competing financial interest.

■ ACKNOWLEDGMENTS

The financial support from Universiti Teknologi MARA through Synergy 2021 Grant 600-TNCPI 5/3/DDF (FKK) (009/2021) and 600-RMC/GPM LPHD 5/3 (088/2022) and from Universiti Sains Malaysia through Research University Grant (RUI) 1001.PJKIMIA.8014128 is greatly acknowledged.

■ REFERENCES

(1) Azmi, A.; Sata, S. A.; Rohman, F. S.; Aziz, N. Dynamic Optimization of Low-Density Polyethylene Production in Tubular Reactor under Thermal Safety Constraint. *Chem. Ind. Chem. Eng. Q.* **2021**, *27*, 85−97.
(2) Buchelli, A.; Call, M. L.; Brown, A. L.; Bird, A.; Hearn, S.; Hannon, J. Modeling Fouling Effects in LDPE Tubular Polymerization Reactors. 1. Fouling Thickness Determination. *Ind. Eng. Chem. Res.* **2005**, *44*, 1474−1479.
(3) Awad, M. M.*Fouling of Heat Transfer Surfaces*; INTECH Open Access Publisher: London, 2011.
(4) Bott, T. R.*Fouling of Heat Exchangers*; Elsevier, 1995, DOI: 10.1016/B978-044482186-7/50017-8.
(5) Thulukkanam, K.*Heat Exchanger Design Handbook*, 1st ed.; CRC Press: Boca Raton, 2000, DOI: 10.1201/9781420026870.
(6) Shah, R. K.; Sekuli, D. P.*Fundamentals of Heat Exchanger Design*; John Wiley & Sons: Hoboken, 2003, DOI: 10.1002/9780470172605.
(7) Ibrahim, H. A.H.*MATLAB - A Fundamental Tool for Scientific Computing and Engineering Applications - Volume 3*; Intech: Rijeka, 2012.
(8) Azmi, A.; Abdul Sata, S.; Rohman, F. S.; Aziz, N. Optimization Studies of Low-Density Polyethylene Process: Effect of Different Interval Numbers. *Chem. Prod. Process. Model.* **2020**, *15*, 20190125.
(9) Rohman, F. S.; Muhammad, D.; Murat, N. M.; Azmi, A. Application of Feed Forward Neural Network for Fouling Thickness Estimation in Low Density Polyethylene Tubular Reactor. *Mater. Today: Proc.* **2022**, *63*, S95−S100.
(10) Kiparissides, C.; Verros, G.; Pertsinidis, A.; Goossens, I. On-Line Parameter Estimation in a High-Pressure Low-Density Polyethylene Tubular Reactor. *AIChE J.* **1996**, *42*, 440−454.
(11) Fries, S.; Castañeda-Zúñiga, D. M.; Duchateau, J.; Neuteboom, P.; Porras, C. T.; Busch, M. Fouling in the High Pressure LDPE Process: Experimental and Computational Investigation Approach. *Macromol. Symp.* **2016**, *360*, 78−86.
(12) Azmi, A.; Sata, S. A.; Rohman, F. S.; Aziz, N. Melt Flow Index of Low-Density Polyethylene Determination Based on Molecular Weight and Branching Properties. *J. Phys.: Conf. Ser.* **2019**, *1349*, No. 012094.
(13) Azmi, A.; Rohman, F. S.; Idris, I.; Zainol, M. M. Sensitivity Study of Input Parameters in the Industrial Low Density Polyethylene Tubular Reactor. *Mater. Today: Proc.* **2022**, *63*, S195−S202.
(14) Azmi, A.; Sudibyo, S.; Sata, S. A.; Aziz, N. Model Based Simulation and Optimization of Industrial Tubular Reactors for High Pressure Low Density Polyethylene Production. *AIP Conf Proc.* **2018**, *2024*, No. 020065.
(15) Piche, S.; Sayyar-Rodsari, B.; Johnson, D.; Gerules, M. Nonlinear Model Predictive Control Using Neural Networks. *IEEE Control Syst.* **2000**, *20*, 53−62.
(16) Kiparissides, C.; Krallis, A.; Meimaroglou, D.; Pladis, P.; Baltsas, A. From Molecular to Plant-Scale Modeling of Polymerization Processes: A Digital High-Pressure Low-Density Polyethylene Production Paradigm. *Chem. Eng. Technol.* **2010**, *33*, 1754−1766.
(17) Skålén, S.; Josefsson, F.; Ihrström, J. Nonlinear MPC for Grade Transitions in an Industrial LDPE Tubular Reactor. *IFAC-PapersOnLine* **2016**, *49*, 562−567.
(18) Zavala, V. M.; Biegler, L. T. Optimization-Based Strategies for the Operation of Low-Density Polyethylene Tubular Reactors: Nonlinear Model Predictive Control. *Comput. Chem. Eng.* **2009**, *33*, 1735−1746.
(19) Azmi, A.; Aziz, N. Comparison Study of Model Based Industrial Low-Density Polyethylene Production in Tubular Reactor. *Chem. Eng. Trans.* **2017**, *56*, 751−756.
(20) Schoukens, J.; Ljung, L. Nonlinear System Identification: A User-Oriented Road Map. *IEEE Control Syst.* **2019**, *39*, 28−99.
(21) Schoukens, M.; Tiels, K. Identification of Block-Oriented Nonlinear Systems Starting from Linear Approximations: A Survey. *Automatica* **2017**, *85*, 272−292.
(22) Shafiee, G.; Arefi, M. M.; Jahed-Motlagh, M. R.; Jalali, A. A. Nonlinear Predictive Control of a Polymerization Reactor Based on Piecewise Linear Wiener Model. *Chem. Eng. J.* **2008**, *143*, 282−292.
(23) Janczak, A. *Identification of Nonlinear Systems Using Neural Networks and Polynomial Models*, 1st ed.; Springer Berlin: Heidelberg, 2005, pp. 310.
(24) Pearson, R. K.; Pottmann, M. Gray-Box Identification of Block-Oriented Nonlinear Models. *J. Process Control* **2000**, *10*, 301−315.
(25) Study of Different Nonlinear Models and Optimizers for Model Predictive Control in Methyl Tertiary Butyl Ether Reactive Distillation Column,Thesis; USM: Nibong Tebal, 2018.
(26) Kadlec, P.; Gabrys, B.; Strandt, S. Data-Driven Soft Sensors in the Process Industry. *Comput. Chem. Eng.* **2009**, *33*, 795−814.
(27) Abeykoon, C. Design and Applications of Soft Sensors in Polymer Processing: A Review. *IEEE Sens. J.* **2018**, *19*, 2801−2813.
(28) Asteasuain, M.; Tonelli, S. M.; Brandolin, A.; Bandoni, J. A. Dynamic Simulation and Optimisation of Tubular Polymerisation Reactors in GPROMS. *Comput. Chem. Eng.* **2001**, *25*, 509−515.
(29) Brandolin, A.; Lacunza, M. H.; Ugrin, P. E.; Capiati, N. J. High Pressure Polymerization of Ethylene. an Improved Mathematical Model for Industrial Tubular Reactors. *Polym. React. Eng.* **1996**, *4*, 193−241.
(30) Cioffi, M.; Hoffmann, A. C.; Janssen, L. P. B. M. Reducing the Gel Effect in Free Radical Polymerization. *Chem. Eng. Sci.* **2001**, *56*, 911−915.
(31) Agrawal, N.; Rangaiah, G. P.; Ray, A. K.; Gupta, S. K. Multi-Objective Optimization of the Operation of an Industrial Low-Density Polyethylene Tubular Reactor Using Genetic Algorithm and Its Jumping Gene Adaptations. *Ind. Eng. Chem. Res.* **2006**, *45*, 3182−3199.
(32) Azmi, A.; Aziz, N. Simulation Studies of Low-Density Polyethylene Production in a Tubular Reactor. *Procedia Eng* **2016a**, *148*, 1170−1176.
(33) Muhammad, D.; Ahmad, Z.; Aziz, N. Modeling and Nonlinearity Studies of Low Density Polyethylene (LDPE) Tubular Reactor. *Mater. Today: Proc.* **2018**, *5*, 21612−21619.
(34) Bokis, C. P.; Ramanathan, S.; Franjione, J.; Buchelli, A.; Call, M. L.; Brown, A. L. Physical Properties, Reactor Modeling, and

Polymerization Kinetics in the Low-Density Polyethylene Tubular Reactor Process. *Ind. Eng. Chem. Res.* **2002**, *41*, 1017−1030.
(35) Azmi, A.; Aziz, N. Low Density Polyethylene Tubular Reactor Modeling: Overview of the Model Developments and Future Directions. *Int. J. Appl. Eng. Res.* **2016b**, *11*, 9906−9913.
(36) Azmi, A.; Aziz, N.Effect of Initiator Concentration to Low-Density Polyethylene Production in a Tubular Reactor. In *IOP Conference Series: Materials Science and Engineering*; Institute of Physics Publishing, 2016; Vol. *162*. DOI: 10.1088/1757-899X/162/1/012023.
(37) Rokudai, M.; Okada, T. Characterization of Low-Density Polyethylenes and Relationships among Melt Index, Density and Molecular Structural Parameters. *J. Sor. Rheol.* **1980**, *8*, 154−160.
(38) Dietrich, M. L.; Sarmoria, C.; Brandolin, A.; Asteasuain, M. LDPE Production in Tubular Reactors: Comprehensive Model for the Prediction of the Joint Molecular Weight-Short (Long) Chain Branching Distributions. *Ind. Eng. Chem. Res.* **2019**, *58*, 4412−4424.
(39) Bremner, T.; Rudin, A.; Cook, D. G. Melt Flow Index Values and Molecular Weight Distributions of Commercial Thermoplastics. *J. Appl. Polym. Sci.* **1990**, *41*, 1617−1627.
(40) Lacunza, M. H.; Ugrin, P. E.; Brandolin, A.; Capiati, N. J. Heat Transfer Coefficient in a High Pressure Tubular Reactor for Ethylene Polymerization. *Polym. Eng. Sci.* **1998**, *38*, 992−1013.
(41) Hussain, M. A. Review of the Applications of Neural Networks in Chemical Process Control — Simulation and Online Implementation. *Eng. Appl. Artif. Intell.* **1999**, *13*, 55−68.
(42) Pirdashti, M.; Curteanu, S.; Kamangar, M. H.; Hassim, M. H.; Khatami, M. A. Artificial Neural Networks: Applications in Chemical Engineering. *Rev. Chem. Eng.* **2013**, *29*, 205−239.
(43) Uddin, F.; Tufa, L. D.; Maulud, A. S. Consistent and Effective Nonlinearity Index and Its Application on Model Predictive Controller Performance Deterioration. *Ind. Eng. Chem. Res.* **2018**, *57*, 14596−14606.
(44) May, R.; Dandy, G.; Maier, H.*Artificial neural networks-methodological advances and biomedical applications*; InTechOpen, 2011; pp.16004.
(45) Khaled, N.; Pattel, B.*Practical Design and Application of Model Predictive Control: MPC for MATLAB and Simulink Users*; Elsevier, 2018.
(46) Muhammad, D.; Ahmad, Z.; Aziz, N. Modeling of Low Density Polyethylene Tubular Reactor Using Nonlinear Block-Oriented Model. *Mater. Today: Proc.* **2021**, *42*, 39−44.
(47) Seborg, D. E.; Edgar, T. F.; Mellichamp, D. A.; Wiley, H.*Process Dynamics and Control*, 2nd ed; Wiley: New York, 2008.
(48) Jacob, N. C.; Dhib, R. Unscented Kalman Filter Based Nonlinear Model Predictive Control of a LDPE Autoclave Reactor. *J. Process Control* **2011**, *21*, 1332−1344.
(49) Ohshima, M.; Ohno, H.; Hashimoto, I.; Sasajima, M.; Maejima, M.; Tsuto, K.; Ogawa, T. Model Predictive Control with Adaptive Disturbance Prediction and Its Application to Fatty Acid Distillation Column Control. *J. Process Control* **1995**, *5*, 41−48.

https://doi.org/10.1021/acsomega.2c03078
ACS Omega 2022, 7, 39648−39661